Journal of Biomedical Optics

SPIEDigitalLibrary.org/jbo

Effects of tissue water content on the propagation of laser light during low-level laser therapy

Soogeun Kim
Sungho Shin
Sungho Jeong

SPIE

Effects of tissue water content on the propagation of laser light during low-level laser therapy

Soogeun Kim, Sungho Shin, and Sungho Jeong*
Gwangju Institute of Science and Technology, School of Mechatronics, 1 Oryong-dong Buk-gu, Gwangju 500-712, Republic of Korea

Abstract. This work reports that the laser fluence rate inside porcine skin varied notably with the change of tissue water content under the same laser irradiation conditions. The laser fluence rate inside skin tissue samples with varying water content was measured using an optical fiber sensor, while the target was irradiated either by a low-level 635 or 830 nm laser (50 mW/cm^2). It was demonstrated that the distribution of laser fluence rate inside the target is strongly affected by tissue water content and its profile is determined by the water content dependency of optical properties at the laser wavelength. [DOI: 10.1117/1.JBO.20.5.051027]

Keywords: low-level laser therapy; water content; tissue; skin; optical property; light propagation.

Paper 140554SSRR received Aug. 31, 2014; accepted for publication Dec. 31, 2014; published online Jan. 22, 2015.

1 Introduction

The use of low-level lasers for therapeutic purpose [low-level laser therapy (LLLT)] has been widely investigated over the past decades and is acknowledged as being effective in certain areas of treatment, such as wound healing,[1] pain reduction,[2] anti-inflammation,[3] nerve regeneration,[4] etc. In LLLT, therapeutic effects are known to depend on the absorption of laser energy by a therapeutic target, which is typically assumed to be influenced by laser irradiation parameters, such as irradiance, irradiation time, and wavelength. In general, when laser energy absorption was insufficient, little therapeutic effects were observed, whereas too much laser energy caused negative suppressing effects.[5–11] For example, Bjordal et al.[6] reported that there existed an optimal irradiance range for pain reduction in chronic joint disorders, which depended on the therapeutic target (finger, toe, knee, etc.) and laser wavelength. For wound healing, Demidova-Rice et al.[7] determined a biphasic dose response curve of 635 nm light, which had a maximum positive effect at the energy density of 2 J/cm^2. In terms of laser wavelength, they reported that 820 nm showed better results than 635, 670, and 720 nm for the same energy density of 1 J/cm^2.

Although the propagation and absorption of laser light in a biological tissue is primarily governed by the laser irradiation parameters, it can also be affected by tissue condition changes even under the same laser irradiation conditions. One of the crucial tissue conditions is tissue water content. Earlier studies showed that the optical properties (absorption and scattering coefficients) of biological tissue varied substantially with the change of tissue water content.[12–16] For example, Cilesiz and Welch[12] reported that the absorption coefficient of the human aorta increased by ~35% for 490 and 515 nm wavelengths and ~42% for 630 nm wavelength when native human aorta was dehydrated by 50 to 90%. The authors also reported that the reduced scattering coefficient of the same sample increased by ~9% due to dehydration for all three wavelengths. However, from the study of dorsal sections of full-thickness rat skin, Rylander et al.[16] reported that dehydration could reduce light scattering in collagenous and cellular tissue. Noting that the optical properties of biological tissue were affected by dehydration, dehydration was also adopted as a method to induce variation in tissue optical property. For example, dehydration by air-immersion[16] or agent-immersion[17] was reported to enhance optical clearing by reducing light scattering in tissue.

On the other hand, the water content of human skin is known to change significantly between individuals, between body parts, or even with time for the same body part. For instance, Nakagawa et al.[18] reported that the average water content of forearm skin of the elderly (mean age: 64) was 5.8% higher than that of young people (mean age: 21) and also that the average water content in forearm skin of healthy male increased by 2.3% in the afternoon from that in the morning. Similarly, the water fraction of women breast skin was reported to vary up to 60% among individuals.[19] It was also reported that the relative water content of cheek was about twice higher than that of forearm and knee for the same person, which was attributed to the difference in stratum corneum thickness.[20]

Therefore, as the patient or target skin for LLLT is changed, it is likely that the optical properties of the target also change due to water content change as reported in the above studies, which in turn will result in a difference in laser light propagation and absorption even under the same laser irradiation conditions. While the administration of an optimum laser dose to a target skin is known to be critical in achieving desired therapeutic effects during LLLT, little information is available in the literature on how the variation of absorption and scattering coefficients due to water content change of the target affects the propagation of laser light.

In this work, the effects of water content on the distribution of laser light within biological tissue during low-level laser irradiation are investigated using visible (635 nm) and infrared (830 nm) lasers. It is demonstrated that the distribution of laser fluence rate measured along the laser beam propagation

*Address all correspondence to: Sungho Jeong, E-mail: shjeong@gist.ac.kr

0091-3286/2015/$25.00

direction differs with respect to tissue water content as well as laser wavelength. Based on numerical calculation results, it is discussed how the induced variations in absorption and scattering coefficients as a result of tissue water content change affect the fluence rate distribution inside tissue.

2 Materials and Methods

2.1 *Sample Preparation*

For experiments, porcine dorsal skin was used as the sample because of its similarity in structural characteristics to human skin.[21,22] The porcine skin sample was obtained from a local abattoir immediately after postmortem and stored in a saline solution at 4°C to minimize dehydration and structural change until measurement. All measurements using the porcine skin sample (thickness ≈ 4 mm) were conducted at room temperature within 12 h from the collection.

The water content of a porcine skin sample, w_t (wt.%), was estimated using the following equation:

$$w_t = \frac{M_{\text{wet}} - M_{\text{dry}}}{M_{\text{wet}}} \times 100, \tag{1}$$

where M_{wet} is the mass of either a native or partially dehydrated sample (g) and M_{dry} is the mass of a dehydrated sample (g). The mass of dehydrated porcine skin (M_{dry}) was measured after dehydrating the native porcine skin at 50°C for 30 min using a moisture analyzer (MB45, Ohaus Corp.). Based on Eq. (1), the water content of native porcine skin was estimated to be ~37 wt.%. The measured water content of 37 wt.% for native porcine skin appeared lower than the values reported in other studies (60 to 75 wt.%) for human and porcine skins.[18,23,24] The reason for the relatively low water content in this study may be attributed to the difference in drying conditions. The water in human skin is customarily classified into three types: tightly bound water (0 to 7 wt.%), bound water (7 to 35 wt.%), and free water (above 35 wt.%).[25] While free water is known to be readily removed in natural or air-dry conditions, earlier studies showed that the bound water could be removed only after significant dehydration, such as drying at 147°C for 50 h,[23] 30 to 40°C for 140 h,[24] or 100°C for 2 h,[26] which significantly exceeded our drying condition (50°C for 30 min). Thus, it is considered that a significant portion of bound water remained after dehydration in the porcine skin samples in this study. Provided that the bound water content of ~30 wt.% is accounted for the samples in this study, the actual water content may rise to ~57 to 67 wt.%. However, since the content of bound water was not confirmed, the water content of the samples used in this study was computed by Eq. (1) using the measured M_{dry} value, which resulted in the water content range of 19 to 37 wt.%, and was used throughout this paper.

2.2 *Laser Irradiation Unit*

Two different continuous wave diode lasers with wavelengths of 635 nm (S1FC635, Thorlabs Inc.) and 830 nm (WSLP-830-050m-M-PD, Wavespectrum Laser Inc.) were used for the irradiation of samples because these wavelengths are frequently employed in LLLT. Both laser beams were collimated using a collimating lens (C230TM-B, Thorlabs Inc.) as shown in Fig. 1. The radii of collimated beams (w_0) of the 635 and 830 nm lasers were 1 and 1.1 mm, respectively. To match

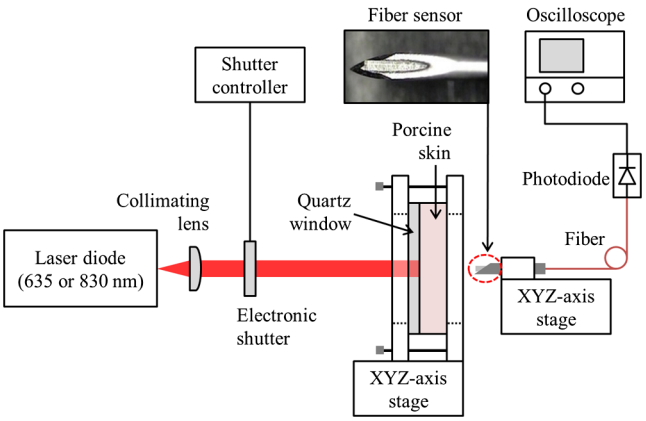

Fig. 1 Schematic of the experimental setup for fluence rate measurement.

the irradiances of both lasers on the sample surface at ~50 mW/cm^2, the irradiance level typically used in LLLT for pain reduction[6] and anti-inflammation,[27] the powers of the 635 and 830 nm lasers were set to 1.6 and 1.9 mW, respectively. The irradiation time was controlled with an electronic shutter and set to 20 s for all measurements.

2.3 *Fluence Rate Measurement*

While the sample surface was irradiated by the collimated laser beam (635 or 830 nm), the fluence rate inside the porcine skin along the laser beam propagation direction was measured at varying depths using an optical fiber sensor. The optical fiber sensor was fabricated as shown in Fig. 1 by inserting a commercial multimode optical fiber (M42L02, Thorlabs Inc.) into a hollow metal needle (outer diameter = 311 μm, inner diameter = 159 μm, length = 1.2 cm, tip angle = 20 deg) and gluing the surface of fiber cladding and the inner surface of the needle with epoxy resin. The fluence rate was measured over the depth range of 0.5 to 3 mm with a 0.5 mm interval by advancing the optical fiber sensor toward the sample surface. To prevent bulging of the sample surface while advancing the optical fiber sensor, a quartz window (thickness = 1 mm) was placed onto the sample surface and then the sample was clamped at both sides using two hollow acrylic plates (see Fig. 1). The depth of the optical fiber sensor from the sample surface was precisely calibrated with respect to the bottom surface of the quartz using translation stages. The light collected by the optical fiber sensor was measured with a photodiode (DET36A, Thorlabs Inc.), whose output voltage signal, S (V), is expressed by[28]

$$S = A \cdot P_1 \cdot P_2 \cdot \Phi, \tag{2}$$

where A ($= \pi r_c^2$, cm^2) is the cross-sectional area of a fiber core with a radius r_c (cm), $P_1 = (1 - \cos\theta_c)/2$ is the ratio of fiber acceptance angle (θ_c) to the entire solid angle (4π), P_2 is photodiode responsivity (V/W), which varies with laser wavelength, and Φ is the fluence rate (W/cm^2). By using Eq. (2), the fluence rate at each depth was estimated from the measured voltage signal.

2.4 *Optical Property Measurement*

The optical properties (absorption and reduced scattering coefficients) of porcine skin at varying water content conditions were measured for both laser wavelengths as follows. First, the total reflectance and transmittance of each water content sample were measured using a double-integrating sphere (AvaSphere-30, Avantes, port diameter = 6 mm).[29] Then, from the measured total reflectance and transmittance data, the optical properties were estimated using an inverse adding-doubling program.[30] In a double-integrating sphere measurement, the sample thickness was recommended to be ~1/10 of the port diameter or smaller to reduce edge loss.[31] The thickness of native sample for optical property measurement was ~700 μm as measured with digital vernier calipers (CD-20CP, Mitutoyo Corp.), which, however, decreased with dehydration to ~680, 660, 630, and 600 μm at the water content of 34, 31, 28, and 25 wt.%, respectively. Below 25 wt.%, the sample thickness showed little change. In addition, the edge loss compensation function of the inverse adding-doubling program was applied for the optical property calculation.

The measurement of optical properties was carried out for samples with the water content range of 19 to 37 wt.% with a 3 wt.% interval. For each water content condition, three samples were tested and each sample was measured three times. The results from three test samples are presented by their average and relative standard deviation.

2.5 *Calculation of Fluence Rate*

The fluence rate of incident laser beam inside the porcine skin samples was also calculated using the diffusion equation for comparison with experimental data. For samples like skin tissue for which scattering dominates over absorption, the propagation of laser light can be reasonably described by the diffusion equation, a simplified form of the radiative transfer equation. Under the conditions of time-independent state, cylindrical symmetry, and normally incident collimated beam, the diffusion equation is expressed by[32]

$$\mu_a \Phi_d(r,z) - D\nabla^2 \Phi_d(r,z) = (3D\mu_t g + 1)\mu_s \Phi_{ri}(r,z), \quad (3)$$

where $\Phi_d\ (r,z)$ is the diffuse fluence rate (W/m^2), g is the anisotropy factor incorporating the effects of directionally dependent scattering, μ_a and μ_s are the absorption and scattering coefficients (m^{-1}), $\mu_t = \mu_a + \mu_s$ is the attenuation coefficient (m^{-1}), and $D = [3(\mu_a + \mu_s\prime)]^{-1}$ is the diffusion coefficient, where the reduced scattering coefficient (m^{-1}) is defined by $\mu_s\prime \equiv \mu_s\ (1-g)$. For a laser beam with nearly uniform spatial profile, the reduced incident fluence rate, $\Phi_{ri}\ (r,z)$ (W/m^2), is expressed by

$$\Phi_{ri}(r,z) = (1-R)\frac{P}{\pi w_0^2}\exp(-\mu_t z) \quad \text{at} \quad r \le w_0, \quad (4)$$

$$\Phi_{ri}(r,z) = 0 \quad \text{at} \quad r > w_0, \quad (5)$$

where R is the specular reflectance off the air/tissue surface at normal incidence and P and w_0 are the laser power (W) and beam radius (m) at the tissue surface, respectively.

At the tissue surface where the diffusion approximation does not hold, the following refractive index mismatched boundary condition was applied:[33]

$$\Phi_d(r,z) - 2C_R D\frac{\partial \Phi_d(r,z)}{\partial z} + 6C_R D\mu_s g\Phi_{ri}(r,z) = 0, \quad (6)$$

where C_R relates to the internal reflection at the interface and can be approximated to be[33]

$$C_R = 1.6896 - 4.90466n + 4.33904n^2 - 0.13755n^3, \quad (7)$$

where n is the relative refractive index representing the ratio of tissue refractive index to that of the ambient medium. In this study, $g = 0.86$,[34] $R = 0.023$, and $n = 1.36$[35] were utilized for calculation.

3 Results and Discussion

Figure 2 shows the absorption (μ_a) and reduced scattering ($\mu_s\prime$) coefficients of the porcine skin measured at varying water content conditions for the 635 and 830 nm wavelengths. It is shown that the μ_a of native porcine skin sample (37 wt.%) was measured to be 0.39 and 0.68 cm^{-1} for 635 and 830 nm, respectively. μ_a values of porcine skin reported in earlier studies were ~0.5 cm^{-1} in 600 to 850 nm regime[24] or 0.7 and 1.6 cm^{-1} at 633 and 850 nm,[36] respectively. Compared to these results, the absorption coefficients measured in this study are considered to lie in an acceptable range. Contrary to that the absorption of biological tissue at 830 nm is typically lower than at 635 nm in the optical window,[36] Fig. 2(a) shows that μ_a at 830 nm wavelength is higher than that at 635 nm wavelength, which is understood to be attributed to the absence of blood in the *in vitro*

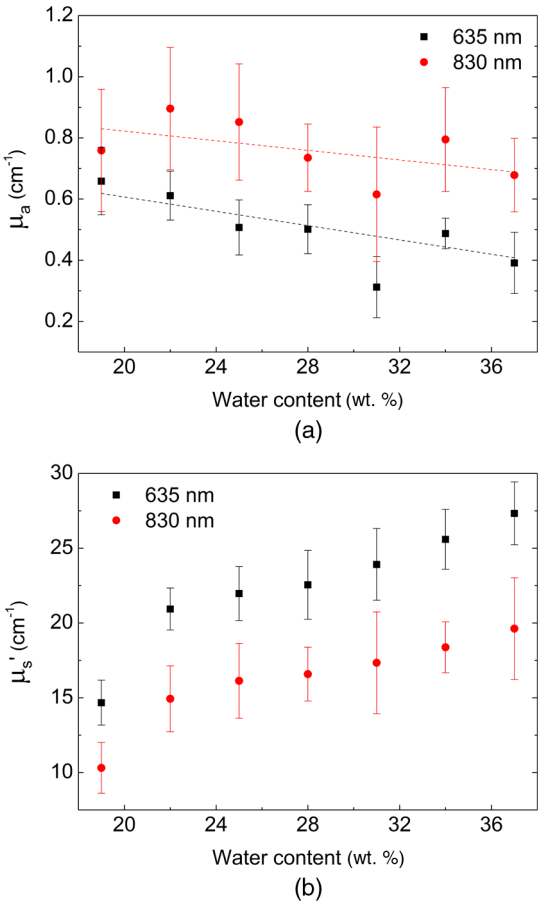

Fig. 2 (a) Absorption coefficient (μ_a) and (b) reduced scattering coefficient ($\mu_s\prime$) of porcine skin measured at varying water content.

sample because light absorption by blood (specifically hemoglobin) is stronger at a 635 nm wavelength.[32] Earlier study for the absorption of *in vitro* porcine skin dermis sample also reported that μ_a at a 850 nm wavelength (1.6 cm^{-1}) was higher than that at a 633 nm wavelength (0.7 cm^{-1}).[36] Note that μ_a of the 635 nm wavelength in Fig. 2(a) shows a clear tendency of increase for decreasing tissue water content. For the 830 nm wavelength, although the data points show much greater relative standard deviation and poorer consistency than the 635 nm wavelength case, a tendency of slight increase is still observable as the tissue water content decreases. The observed increase of μ_a for decreasing water content may be attributed to denser packing of collagen fibers during shrinkage of the tissue sample by dehydration.[14] On the other hand, μ_s' of the porcine skin in Fig. 2(b) shows nearly the same pattern for both wavelengths. μ_s' decreased gradually as the water content decreased from the native condition of 37 wt.% to ~22 wt.% but dropped rather rapidly as the water content decreased from 22 to 19 wt.%. The observed decrease of μ_s' as a result of dehydration of skin tissue agrees with an earlier report.[16]

Figure 3 shows the measured and calculated fluence rate distribution along the depth of porcine skin samples for different water content conditions. Each experimental data point represents the average and relative standard deviation from nine measurements on the same sample. The average difference between measured and calculated fluence rates at 635 nm wavelength was ~4.5% (maximum = 13.5% at 1.5 mm depth for 25 wt.% sample) and that at 830 nm wavelength was ~5.5%

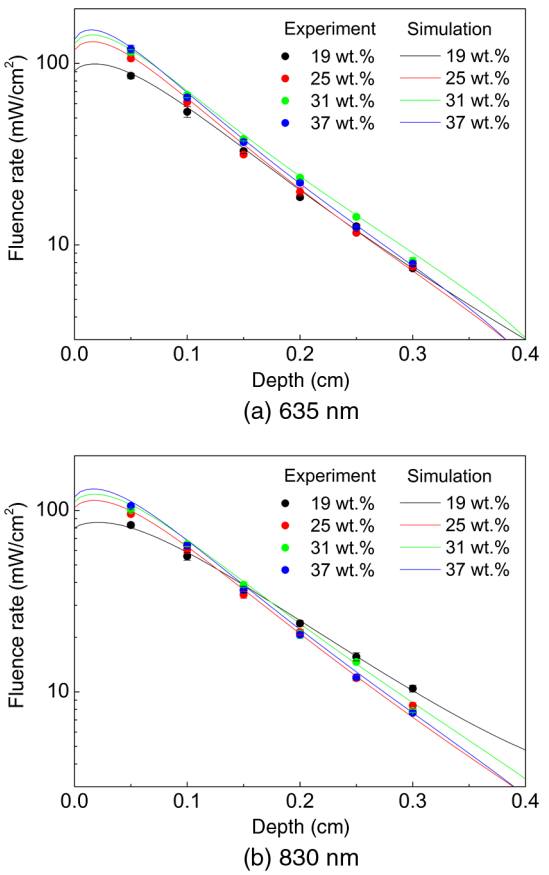

Fig. 3 Fluence rate profiles of the (a) 635-nm and (b) 830-nm lasers along the laser beam propagation direction in different water content samples.

(maximum = 14.5% at 2 mm depth for 31 wt.% sample). First of all, the results show that the fluence rate and its distribution changed notably as tissue water content changed under the same laser irradiation conditions. Note that the irradiance at the sample surface was fixed at 50 mW/cm^2 for all measurements. For biological tissue in which $\mu_s' \gg \mu_a$ is satisfied, it is known that (1) if μ_s' remained constant, an increase of μ_a results in an overall decrease of fluence rate at all depths and (2) if μ_a remained constant, a decrease of μ_s' leads to a decrease of fluence rate at and near the surface but an increase in deeper locations.[37,38] According to this information, the fluence rate at and near the surface should have decreased while that in deeper locations increased as the water contents dropped from 37 to 19 wt.% because μ_s' was also decreased as shown in Fig. 2(b). This expected change in fluence rate distribution was in fact observed in the data for the 830 nm wavelength in Fig. 3(b), where the fluence rate at 0.5 mm depth decreased by maximum 32% while that at 3 mm depth increased by a maximum 25%. The calculated fluence rate also agreed closely with the measured data for this wavelength. Unlike the 830 nm wavelength case, however, the measured and calculated data for the 635 nm wavelength in Fig. 3(a) do not show exactly the same trend. While the fluence rate change at and near the surface showed a trend similar to the 830 nm wavelength case (maximum 31% decrease), that in the deeper locations revealed an unclear pattern.

The observed difference in fluence rate distribution between the 635 and 830 nm wavelengths can be better understood by examining how μ_a and μ_s' affect the fluence rate of both laser wavelengths as the water content of the target tissue changes from 37 to 19 wt.%. For this purpose, taking μ_a and μ_s' of the 37 wt.% sample as the reference values, the influence of μ_a and μ_s' change on the fluence rate distribution was investigated for the following three cases by numerical simulation: (1) μ_s' was changed to that of the 19 wt.% sample while μ_a remained the same (at the 37 wt.% value), (2) μ_a was changed to that of the 19 wt.% sample, while μ_s' remained the same, and (3) both μ_a and μ_s' were changed to those of the 19 wt.% sample, as summarized in Table 1 with the corresponding μ_a and μ_s' values. Figure 4(a) shows the calculation results of $\Phi_{case\,j}/\Phi_{37\,wt.\%}$ for the 635 nm wavelength, where $\Phi_{case\,j}$ represents the fluence rate calculated with one of the three combinations of μ_a and μ_s'. When μ_s' only was changed to that of the 19 wt.% sample as described in the first case (for this case, μ_s' decreased by 47%), $\Phi_{case\,1}/\Phi_{37\,wt.\%,635\,nm}$ became <1.0 at and near the surface but increased gradually >1.0 as the depth

Table 1 Absorption and reduced scattering coefficients used for fluence rate distribution calculation.

	635 nm		830 nm	
	μ_a (cm^{-1})	μ_s' (cm^{-1})	μ_a (cm^{-1})	μ_s' (cm^{-1})
37 wt.% (Reference)	0.39	27.33	0.68	19.62
μ_a and μ_s' of 19 wt.%	**0.66**	**14.67**	**0.76**	**10.31**
Case 1 (μ_s' of 19 wt.%)	0.39	**14.67**	0.68	**10.31**
Case 2 (μ_a of 19 wt.%)	**0.66**	27.33	**0.76**	19.62

Note: Bold values represents the values changed from the reference values at 37 wt.%.

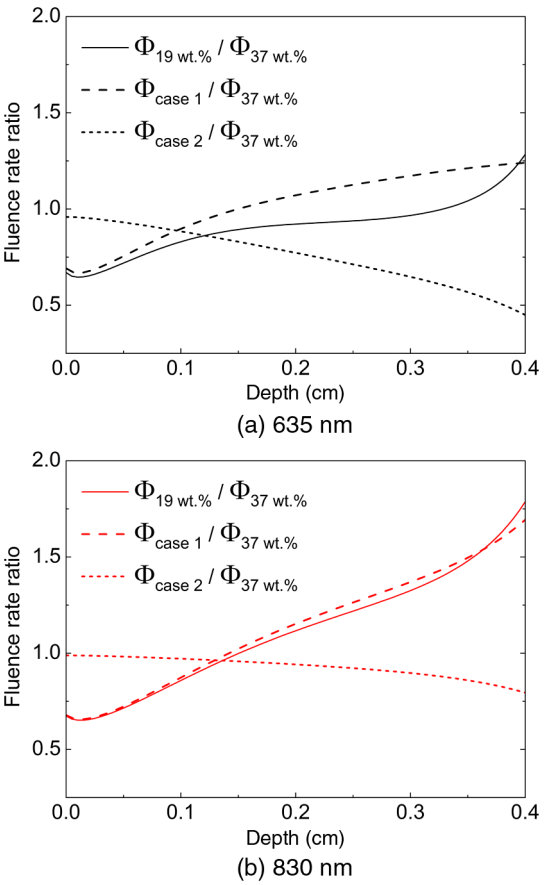

Fig. 4 Effects of the absorption and reduced scattering coefficients on fluence rate ratio profile for the (a) 635 nm and (b) 830 nm wavelengths.

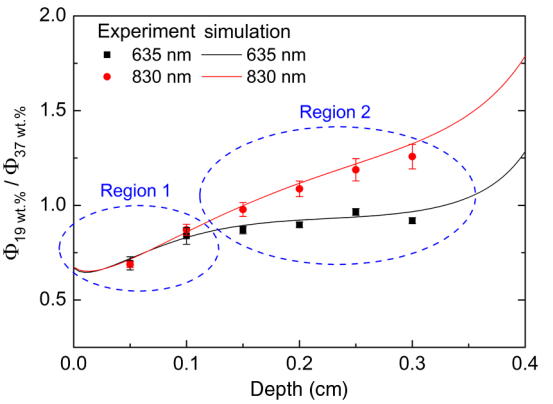

Fig. 5 Dependency of the fluence rate ratio profiles on laser wavelength.

increased. Next, when μ_a only was changed to that of the 19 wt.% sample (μ_a increased by 68%), $\Phi_{case\,2}/\Phi_{37\,wt.\%,635\,nm}$ decreased continuously over the entire depth as expected. Last, when the actual μ_a and $\mu_s\prime$ values of the 19 wt.% sample were used, a distribution curve in between those two previous cases was obtained. The calculation results for case 1 and case 2 of the 830 nm wavelength in Fig. 4(b) show, in principle, the same trends as those of 635 nm wavelength. However, the magnitude of fluence rate of the 830 nm wavelength for the second case decreased only slightly because of the relatively small increase of μ_a (12%), and, thus, $\Phi_{case\,2}/\Phi_{37\,wt.\%,830\,nm}$ showed a much more moderate reduction over the depth. Since the degree of $\mu_s\prime$ decrease of the 830 nm wavelength (48%) as the water content dropped from 37 to 19 wt.% is almost the same as that of the 635 nm wavelength (47%), the combined effects of μ_a and $\mu_s\prime$ change of the 830 nm wavelength resulted in a continuous increase of $\Phi_{19\,wt.\%}/\Phi_{37\,wt.\%,830\,nm}$ over 1.0 in the deep tissue region as observed in Fig. 4(b).

The above-explained difference in fluence rate distribution between the 635 and 830 nm wavelengths is more clearly observed when $\Phi_{19\,wt.\%}/\Phi_{37\,wt.\%}$ of these wavelengths are plotted together as shown in Fig. 5. From Fig. 5, first it is seen that the fluence rate ratio of both wavelengths had almost the same distribution in the region close to the sample surface (for depth $< \sim$1 mm, region 1), over which the fluence rate of 19 wt.% sample was smaller than that of the 37 wt.% sample. Beyond 1 mm depth (region 2), however, the fluence rate ratios of both wavelengths show different trends. For the 635 nm wavelength, the fluence rate of the 19 wt.% sample still remained below that of the 37 wt.% sample and the ratio was almost constant over the entire depth range in the experiments (0.5 to 3 mm). For the 830 nm wavelength, the fluence rate ratio kept increasing almost linearly with respect to depth, which represents that the fluence rate of the 19 wt.% sample in this deeper region became greater than that of the 37 wt.% sample.

In the LLLT point of view, the above results may be interpreted as follows. Assuming that the optimal laser irradiance was determined at the water content condition of the native sample (37 wt.%), (1) provided that the therapeutic target region lies within $\sim$1 mm depth from the surface, the laser irradiance should be increased to achieve the same therapeutic effects regardless of the laser wavelength if the water content of target tissue is lower than the native sample and (2) provided that the therapeutic target region lies beyond $\sim$1 mm depth from the surface, laser irradiance should be changed in consideration of the laser wavelength. That is, for the 635 nm wavelength, the laser irradiance should be kept nearly the same or slightly increased if the water content of target tissue is lower than the native sample, whereas for the 830 nm wavelength, the laser irradiance needs to be reduced to achieve the same therapeutic effects in this deeper region.

4 Conclusion

From the experimental and numerical study of porcine skin irradiated by low-level 635 and 830 nm lasers, it was shown that the fluence rate and its distribution along the laser propagation direction changed notably as the water content of porcine skin was reduced from that of a native sample (37 wt.%) to 19 wt.%. While the fluence rate profile at and near the sample surface was similar between the two wavelength lasers as the water content changed, that in the deeper region became completely different due to the different water content dependency of optical properties. These results suggest that the optimum laser dose for LLLT should be adjusted if the water content of a therapeutic target changed and the adjustment needs to be made in consideration of the laser wavelength as well as the depth of the therapeutic target.

References

1. J. T. Hopkins et al., "Low-level laser therapy facilitates superficial wound healing in humans: a triple-blind, sham-controlled study," *J. Athl. Train.* **39**(3), 223–229 (2004).

2. R. T. Chow, G. Z. Heller, and L. Barnsley, "The effect of 300 mW, 830 nm laser on chronic neck pain: a double-blind, randomized, placebo-controlled study," *Pain* **124**(1–2), 201–210 (2006).
3. R. A. Lopes-Martins et al., "Spontaneous effects of low-level laser therapy (650 nm) in acute inflammatory mouse pleurisy induced by carrageenan," *Photomed. Laser Surg.* **23**(4), 377–381 (2005).
4. D. Gigo-Benato et al., "Low-power laser biostimulation enhances nerve repair after end-to-side neurorrhaphy: a double-blind randomized study in the rat median nerve model," *Lasers Med. Sci.* **19**(1), 57–65 (2004).
5. A. P. Sommer et al., "Biostimulatory windows in low-intensity laser activation: lasers, scanners, and NASA's light-emitting diode array system," *J. Clin. Laser Med. Sur.* **19**(1), 29–33 (2001).
6. J. M. Bjordal et al., "A systematic review of low level laser therapy with location-specific doses for pain from chronic joint disorders," *J. Physiother.* **49**(2), 107–116 (2003).
7. T. N. Demidova-Rice et al., "Low-level light stimulates excisional wound healing in mice," *Lasers Surg. Med.* **39**(9), 706–715 (2007).
8. Y. Y. Huang et al., "Biphasic dose response in low level light therapy," *Dose-Response* **7**(4), 358–383 (2009).
9. H. Chung et al., "The nuts and bolts of low-level laser (light) therapy," *Ann. Biomed. Eng.* **40**(2), 516–533 (2012).
10. T. D. Magrini et al., "Low-level laser therapy on MCF-7 cells: a micro-Fourier transform infrared spectroscopy study," *J. Biomed. Opt.* **17**(10), 101516 (2012).
11. V. P. Wagner et al., "Influence of different energy densities of laser phototherapy on oral wound healing," *J. Biomed. Opt.* **18**(12), 128002 (2013).
12. I. F. Cilesiz and A. J. Welch, "Light dosimetry: effects of dehydration and thermal damage on the optical properties of the human aorta," *Appl. Opt.* **32**(4), 477–487 (1993).
13. V. V. Tuchin et al., "Light propagation in tissues with controlled optical properties," *J. Biomed. Opt.* **2**(4), 401–417 (1997).
14. D. Zhu, Q. Luo, and J. Cen, "Effects of dehydration on the optical properties of *in vitro* porcine liver," *Lasers Surg. Med.* **33**(4), 226–231 (2003).
15. M. H. Khan et al., "Optical clearing of *in vivo* human skin: implications for light-based diagnostic imaging and therapeutics," *Lasers Surg. Med.* **34**(2), 83–85 (2004).
16. C. G. Rylander et al., "Dehydration mechanism of optical clearing in tissue," *J. Biomed. Opt.* **11**(4), 041117 (2006).
17. D. Zhu et al., "Recent progress in tissue optical clearing," *Laser Photon. Rev.* **7**(5), 732–757 (2013).
18. N. Nakagawa, M. Matsumoto, and S. Sakai, "*In vivo* measurement of the water content in the dermis by confocal Raman spectroscopy," *Skin Res. Technol.* **16**(2), 137–141 (2010).
19. A. E. Cerussi et al., "Spectroscopy enhances the information content of optical mammography," *J. Biomed. Opt.* **7**(1), 60–71 (2002).
20. M. Egawa et al., "Regional difference of water content in human skin studied by diffuse-reflectance near-infrared spectroscopy: consideration of measurement depth," *Appl. Spectrosc.* **60**(1), 24–28 (2006).
21. R. M. Lavker et al., "Hairless micropig skin. A novel model for studies of cutaneous biology," *Am. J. Pathol.* **138**(3), 687–697 (1991).
22. N. J. Vardaxis et al., "Confocal laser scanning microscopy of porcine skin: implications for human wound healing studies," *J. Anat.* **190**(4), 601–611 (1997).
23. F. S. Knox, III et al., "Thermal properties calculated from measured water content as a function of depth in porcine skin," *Burns* **12**(8), 556–562 (1986).
24. T. Yu et al., "Quantitative analysis of dehydration in porcine skin for assessing mechanism of optical clearing," *J. Biomed. Opt.* **16**(9), 095002 (2011).
25. E. Berardesca, "EEMCO guidance for the assessment of stratum corneum hydration: electrical methods," *Skin Res. Technol.* **3**(2), 126–132 (1997).
26. J. J. Bulgin and L. J. Vinson, "The use of differential thermal analysis to study the bound water in stratum corneum membranes," *Biochim. Biophys. Acta-Gen. Subj.* **136**(3), 551–560 (1967).
27. A. P. Castano et al., "Low-level laser therapy for zymosan-induced arthritis in rats: importance of illumination time," *Lasers Surg. Med.* **39**(6), 543–550 (2007).
28. S. Kim and S. Jeong, "Effects of temperature-dependent optical properties on the fluence rate and temperature of biological tissue during low-level laser therapy," *Lasers Med. Sci.* **29**(2), 637–644 (2014).
29. J. W. Pickering et al., "Double-integrating-sphere system for measuring the optical properties of tissue," *Appl. Opt.* **32**(4), 399–410 (1993).
30. S. A. Prahl, M. J. van Gemert, and A. J. Welch, "Determining the optical properties of turbid media by using the adding-doubling method," *Appl. Opt.* **32**(4), 559–568 (1993).
31. S. A. Prahl, *Inverse Adding-Doubling for Optical Property Measurements*, Oregon Medical Laser Center, Portland, Oregon (2007).
32. L. V. Wang and H. I. Wu, *Biomedical Optics: Principles and Imaging*, John Wiley & Sons, Hoboken (2007).
33. S. A. Prahl, "Light transport in tissue," PhD Dissertation, The University of Texas at Austin (1988).
34. X. Ma et al., "Bulk optical parameters of porcine skin dermis at eight wavelengths from 325 to 1557 nm," *Opt. Lett.* **30**(4), 412–414 (2005).
35. H. Ding et al., "Determination of refractive indices of porcine skin tissues and intralipid at eight wavelengths between 325 and 1557 nm," *J. Opt. Soc. Am. A* **22**(6), 1151–1157 (2005).
36. A. N. Bashkatov, E. A. Genina, and V. V. Tuchin, "Optical properties of skin, subcutaneous, and muscle tissues: a review," *J. Innov. Opt. Health Sci.* **4**(1), 9–38 (2011).
37. S. Rastegar et al., "A theoretical study of the effect of optical properties in laser ablation of tissue," *IEEE Trans. Biomed. Eng.* **36**(12), 1180–1187 (1989).
38. M. Motamedi et al., "Light and temperature distribution in laser irradiated tissue: the influence of anisotropic scattering and refractive index," *Appl. Opt.* **28**(12), 2230–2237 (1989).

Soogeun Kim is a PhD candidate at the Gwangju Institute of Science and Technology, Republic of Korea. He received a BS degree in mechanical engineering from Yeungnam University in 2004 and an MS degree in mechatronics from Gwangju Institute of Science and Technology in 2007. His research focuses on laser-tissue interaction mechanisms with low and high power lasers and their applications, especially as related to the effect of tissue conditions on laser-tissue interaction mechanisms.

Sungho Shin is a PhD candidate in mechatronics at Gwangju Institute of Science and Technology, Republic of Korea. He received a BS degree in biomedical engineering from Yonsei University in 2012 and an MS degree in the Department of Medical System Engineering from Gwangju Institute of Science and Technology in 2014. His research interests include applications of low and high power lasers for medical diagnostics and therapeutics.

Sungho Jeong is a professor at Gwangju Institute of Science and Technology, Republic of Korea. He received a PhD in mechanical engineering from the University of California at Berkeley in 1997 and worked at Lawrence Berkeley National Laboratory during his doctoral and postdoctoral studies. His research focuses on laser ablation phenomena and their applications, and ongoing research includes application of laser-induced breakdown spectroscopy for thin film solar cell, laser shock peening, and laser interaction with biomedical materials.